

Microstructure and properties of hydrophobic films derived from Fe–W amorphous alloy

Song Wang^{1,2}, Yun-han Ling², Jun Zhang², Jian-jun Wang¹, and Gui-ying Xu¹

1) School of Materials Science and Engineering, University of Science and Technology Beijing, Beijing 100083, China

2) School of Materials Science and Engineering, Tsinghua University, Beijing 100084, China

(Received: 30 October 2013; revised: 16 December 2013; accepted: 17 December 2013)

Abstract: Amorphous metals are totally different from crystalline metals in regard to atom arrangement. Amorphous metals do not have grain boundaries and weak spots that crystalline materials contain, making them more resistant to wear and corrosion. In this study, amorphous Fe–W alloy films were first prepared by an electroplating method and were then made hydrophobic by modification with a water repellent (heptadecafluoro-1,1,2,2-tetradecyl) trimethoxysilane. Hierarchical micro-nano structures can be obtained by slightly oxidizing the as-deposited alloy, accompanied by phase transformation from amorphous to crystalline during heat treatment. The micro-nano structures can trap air to form an extremely thin cushion of air between the water and the film, which is critical to producing hydrophobicity in the film. Results show that the average values of capacitance, roughness factor, and impedance for specific surface areas of a 600°C heat-treated sample are greater than those of a sample treated at 500°C. Importantly, the coating can be fabricated on various metal substrates to act as a corrosion retardant.

Keywords: iron tungsten alloys; amorphous films; hydrophobicity; microstructure; contact angle; capacitance

1. Introduction

Hydrophobic and super-hydrophobic surface treatments on different substrates have attracted considerable interest in both academia and industry because of their potential applications [1–3]. Fabrication of such hydrophobic coatings depends on two prerequisites: (1) the material surface must contain hierarchical micro- and nano-scale structures, and (2) the rough surface must be modified with a special low-surface-energy material [4–5]. It is believed that the micro- and nano-scale roughness, similar to nano-hairs on a lotus leaf, is the key to water repellency and self-cleaning effect. This hierarchical roughness promotes the trapping of air between the water droplet and the surface, thus preventing water from penetrating into the surface [1]. A number of artificial hydrophobic surfaces have been achieved by mimicking surface structures in nature such as the lotus leaf [6] and the butterfly [7]. Many techniques can be employed to fabricate hydrophobic surfaces, such as spin-coating [8], electro-

chemical processes [9], sol-gel processes [10], electrospray [11], chemical vapor deposition (CVD), lithography, chemical etching [12], and so on.

The present investigation proposed a novel and universal method for constructing hierarchical nanostructures on any conductive substrate by electroplating it with an amorphous Fe–W alloy. This amorphous coating can be made hydrophobic by further modification with a water-repelling agent having low surface energy. After heat treatment, a surface coating containing Fe–W micro-nano scale wires and protuberances had been fabricated. The hydrophobicity and corrosion resistance of the coating was characterized by contact angle test, electrochemical measurements, and so on.

2. Experimental

A 2.5 mm-thick copper sheet was selected as the substrate; the copper sheet was cut into 10 mm × 20 mm pieces and polished mechanically using 1500 grit waterproof abrasive sheets to remove surface impurities and oxide/hydro-

Corresponding author: Yun-han Ling E-mail: yhling@mail.tsinghua.edu.cn

© University of Science and Technology Beijing and Springer-Verlag Berlin Heidelberg 2014

xide layers. The samples were then sequentially cleaned with alcohol, deionized via ultrasonication, and dried in air.

In the current paper, a simple electrochemical machining method using a relatively nonpoisonous (heptadecafluoro-1,1,2,2-tetradecyl) trimethoxysilane ethanol solution was used for the fabrication of a hydrophobic surface on the Cu substrate. In the first step, amorphous Fe–W alloy films were prepared on the Cu surfaces by an electroplating method. The bath composition and electroplating conditions for the amorphous Fe–W alloys are presented in Table 1. In the second step, the amorphous samples were subjected to heat treatment that involved heating at $10^{\circ}\text{C}\cdot\text{min}^{-1}$ to 500°C or 600°C for 2 h under a controlled low vacuum atmosphere, and then cooling the samples to room temperature. In the third step, the annealed samples were immersed in the water repellent (heptadecafluoro-1,1,2,2-tetradecyl) trimethoxysilane for 24 h to produce a uniform hydrophobic layer on the surfaces, followed by drying in an oven at 80°C for 3 h.

Table 1. Bath composition and operating conditions for electroplating

Bath reagents and concentrations	$(\text{NH}_3)_2\text{C}_4\text{H}_4\text{O}_6 / (\text{mol}\cdot\text{L}^{-1})$	0.26
	$\text{Na}_2\text{WO}_4\cdot 2\text{H}_2\text{O} / (\text{mol}\cdot\text{L}^{-1})$	0.018–0.036
	$\text{FeSO}_4\cdot 7\text{H}_2\text{O} / (\text{mol}\cdot\text{L}^{-1})$	0.212–0.243
	Electroplating temperature / $^{\circ}\text{C}$	60
Operating conditions	pH (adjusted by H_2SO_4)	4–6
	Current density / $(\text{A}\cdot\text{cm}^{-2})$	0.5
	Electroplating duration / min	5

The surface morphologies and chemical compositions of the obtained samples were investigated by using a field emission scanning electron microscope (FESEM, HITACH S4800) equipped with energy-dispersive spectroscopy (EDS, INCA Energy, Oxford Ins). X-ray diffraction (XRD, D/max 2500, Cu K_{α}) analysis was employed on the samples to determine the crystallinity of the as-deposited samples. The surface roughness of the obtained samples was analyzed by their cyclic voltammetric patterns.

Contact angles were obtained by using the sessile drop method with a JGW-360A optical contact angle system (Midwest-group, China). Distilled water drops were separately placed on each sample surface ($5\ \mu\text{L}/\text{drop}$), and the corresponding contact angles were measured subsequently. Three different regions on the surface were used, and the measured results were averaged to reduce deviation.

The electrochemical corrosion behavior was investigated by electrochemical impedance spectroscopy (EIS) using a Zahner IM6E computer-controlled potentiostat under open-circuit conditions. For these electrochemical measurements,

a three-electrode configuration was designed, in which a sample with an exposed hydrophobic Fe–W alloy test area of $1\ \text{cm}^2$ was used as the working electrode, a platinum electrode as the counter electrode, and a saturated calomel electrode (SCE) as the reference electrode. Prior to EIS measurements, the samples were allowed to stabilize at their open-circuit potential (OCP) for 30 min before the measurements were started. The EIS measurements were carried out using 10 mV peak-to-peak sinusoidal perturbation over a frequency range extending from 100 mHz to 1 MHz at the respective OCPs.

3. Results and discussion

To examine the influence of surface morphology on the hydrophobic nature of the resulting film, FESEM was utilized to capture the surface images at high magnification. Figs. 1(a), 1(b), and 1(c) show the FESEM images of the as-deposited surface and the hydrophobic surfaces with different heat-treatment temperatures, respectively. The XRD results are shown in Fig. 2. Only one peak is found, at the 2θ angle of approximately 42° . The result attests to the amorphous nature of the as-deposited film.

Hierarchical micro-nano structures can be obtained by slight oxidation of the as-deposited alloy accompanied by phase transformation from amorphous to crystalline during heat treatment [13]. A rough, porous structure is observed on the surface of the as-deposited sample. The formation of this rough, porous structure is believed to be related to internal stresses caused by the evolution of hydrogen. Under high magnification it can be seen that the surface is covered by nubby clusters (Fig. 1(b)) and micro-nano scale wires (Fig. 1(c)). Furthermore the nubby clusters exhibit an interesting structure with micro-nano scale protuberances. Such micro-nano scale structures and cavities on the surface play important roles in trapping air [14]. The low surface energy of the materials, as well as the rough micro-nano scale structures on the surface, is crucial for realizing hydrophobicity.

The surface wettability of various substrates was characterized by static water contact angle measurements using $5\ \mu\text{L}$ of water. Fig. 3 shows photographs of water droplets on the surfaces of the hydrophobic samples. The untreated Fe–W alloy surface is hydrophilic. It can be seen that the wettability of the surface is significantly changed after the as-deposited and the annealed samples are modified by the hydrophobic treatment. As shown in Fig. 3, the water contact angles of these samples heat-treated at different temperatures change in a pattern that correlates with the mor-

phologies observed with SEM as shown in Fig. 1. It is found that the surfaces of as-deposited, 500°C annealed, and 600°C annealed samples are hydrophobic with water contact

angles of $(95 \pm 1)^\circ$, $(111 \pm 1)^\circ$, and $(134 \pm 1)^\circ$, respectively. Obviously, the contact angle of the surface increases with the rise of annealing temperature and reaches the high value

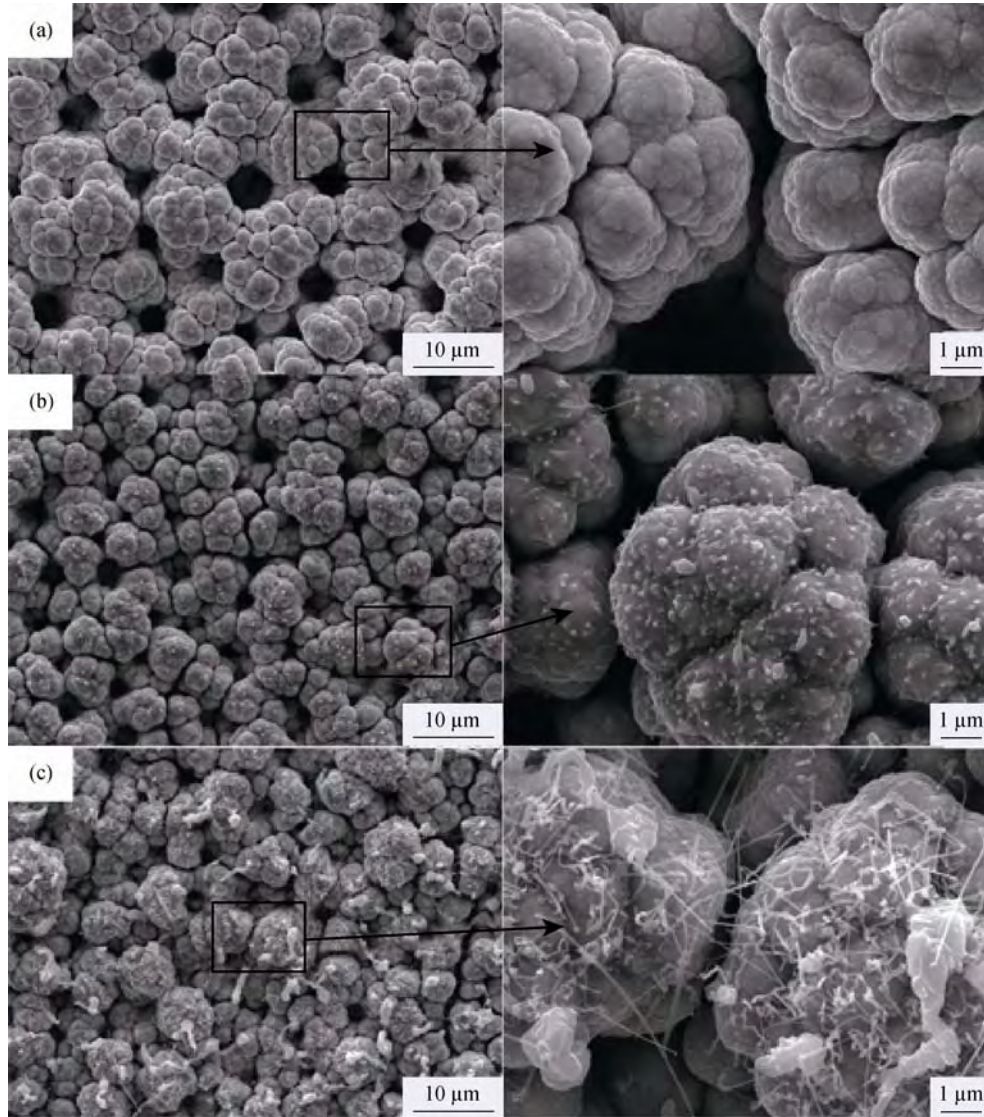


Fig. 1. FESEM images of the as-deposited surface (a) and the hydrophobic surfaces annealed at 500°C (b) and 600°C (c).

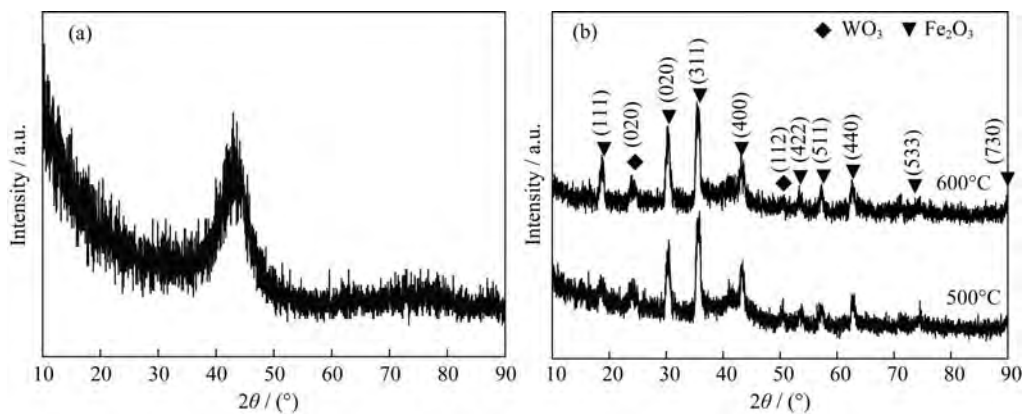


Fig. 2. XRD patterns of the amorphous Fe–W deposition (a) and the annealed films heat-treated at different temperatures (b).

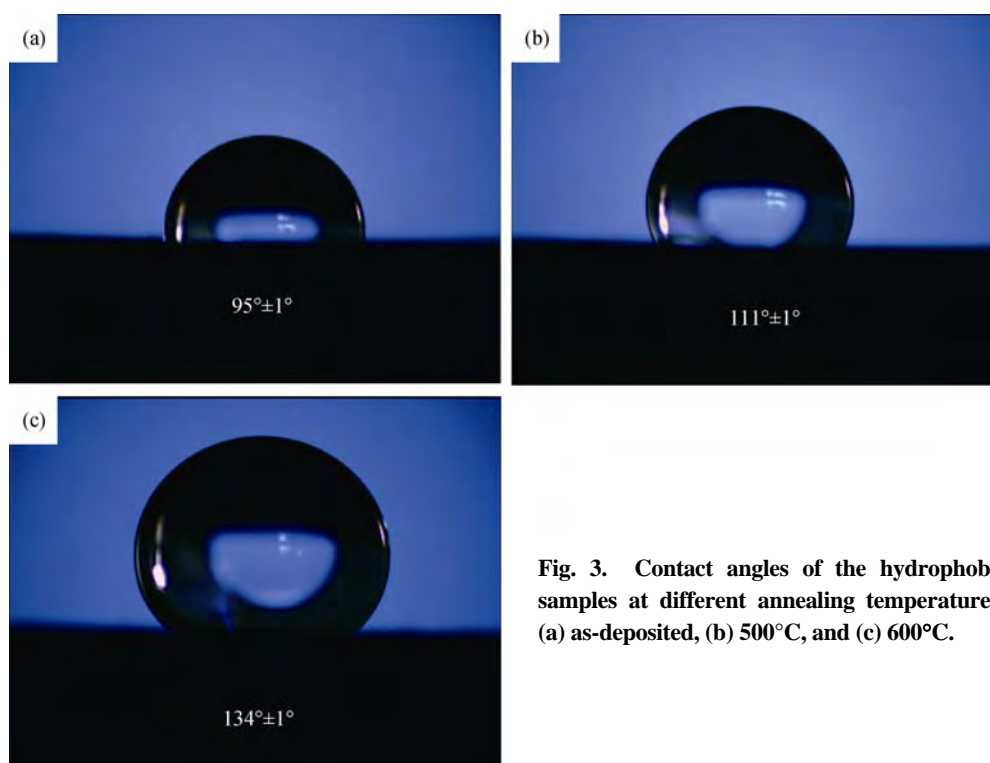


Fig. 3. Contact angles of the hydrophobic samples at different annealing temperatures: (a) as-deposited, (b) 500°C, and (c) 600°C.

of 134° at 600°C. An increase in hydrophobicity could minimize the adhesive interaction between the water drop and the solid surface, hence increasing the contact angle. The contact angle of a hydrophobic film can be significantly increased by making the surface relatively rough, as implied by the Wenzel model. The hydrophobic is strongly dependent on surface roughness and surface energy. These results provide feasibility toward obtaining a hydrophobic surface, and this technique, which supplied these promising results, deserves in-depth investigation.

The roughness of the Fe–W deposition layers annealed at different temperatures can be evaluated by the double layer capacitive change at the electrode/electrolyte interface. A typical voltammetric pattern at different scan rates for the as-annealed Fe–W deposition layer serving as a working electrode is shown in Fig. 4. Curves of charging current versus voltage were recorded with the scan rate ranging from 0.5 to 8 mV·s⁻¹. The charging current at each sweep rate was measured in the middle of the scan range and was plotted as a function of the sweep rate. Linear dependencies of the current on the sweep rate with positive intercepts are observed for both of the studied electrodes, as presented in Figs. 4(b) and 4(d). The positive intercepts are probably related to the presence of ohmic drop effect introduced by grain boundaries inside the sample.

From the slopes, the capacitance of each deposition/electrolyte interface ($C = dq/dE = dI/dv$, where C is the capaci-

tance, q is the electric quantity, E is the voltage, I is the current density, and v is the scan rate) can be estimated. The relative magnitude of the respective roughness factor, R_f , is calculated by assuming the value of 60 μF·cm⁻² for the capacitance of a smooth oxide surface ($R_f = C/60$) [15–16]. Therefore, the average values of capacitance and roughness factor calculated for the 500°C and 600°C annealed Fe–W electrodes are 5172.7 μF·cm⁻², 7047.7 μF·cm⁻² and 82.2, 117.5, respectively, implying that the specific surface areas of the 600°C heat-treated sample are larger than those of the sample treated at 500°C.

The electrochemical impedance test adopted the three-electrode system. Electrochemical impedance plots of the annealed (bare) Fe–W deposition layer and the modified Fe–W deposition layer in 0.1 mol/L NaCl solution are shown in Fig. 5. According to the EIS plots, an obvious change can be observed from the presence of hydrophobicity. As shown in the Fig. 5, the impedance of the hydrophobic Fe–W deposition layer is much higher than that of the unmodified Fe–W deposition layer. The 600°C annealed Fe–W deposition presents a higher impedance for charge transfer. Due to the blocking effect of the film, it is difficult for the electrolyte to sweep into the metallic layer. The electrolyte can only penetrate slowly by zigzagging along tiny gaps in the film [14]. The impedance plots indicated that the modified Fe–W deposition layer has a greater corrosion resistance than the unmodified layer.

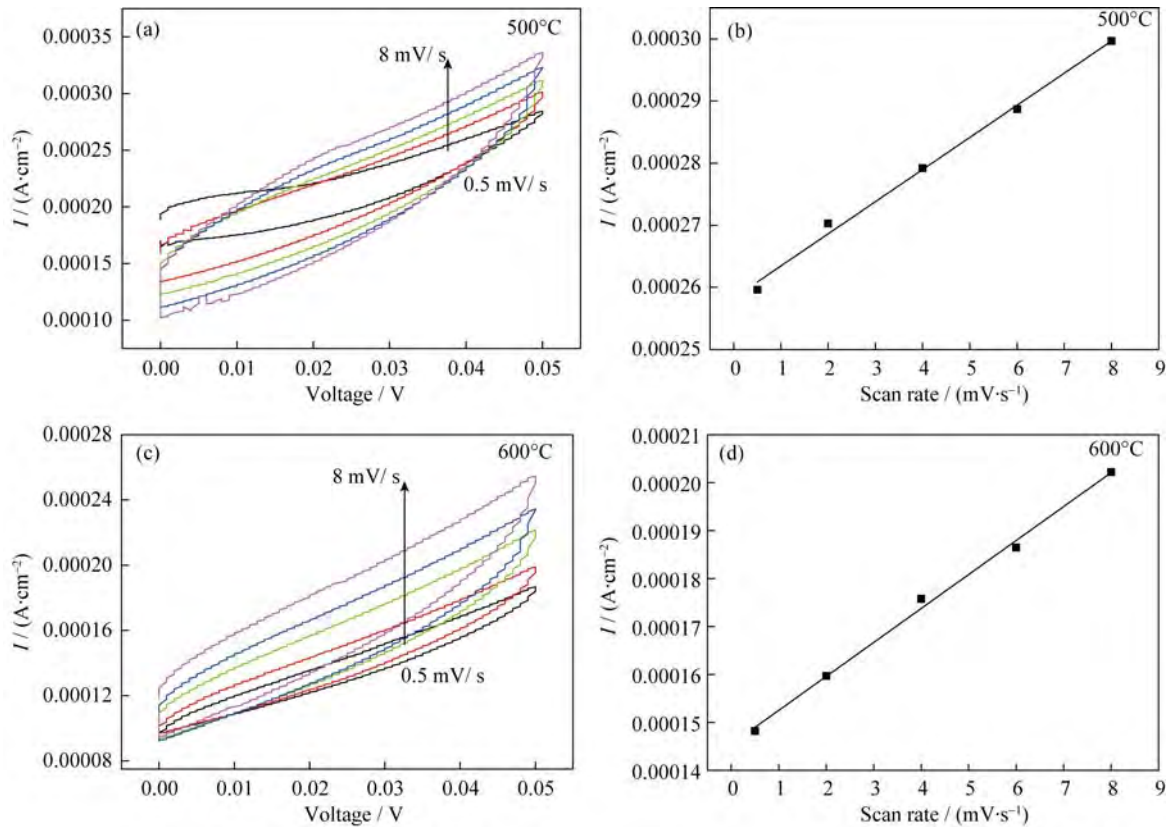


Fig. 4. Surface capacitance characteristics of Fe–W deposition. Cyclic voltammograms at different scan rates in the double-layer region of the Fe–W electrodes annealed at 500°C (a) and 600°C (c); charging current as a function of scan rate for the electrodes annealed at 500°C (b) and 600°C (d).

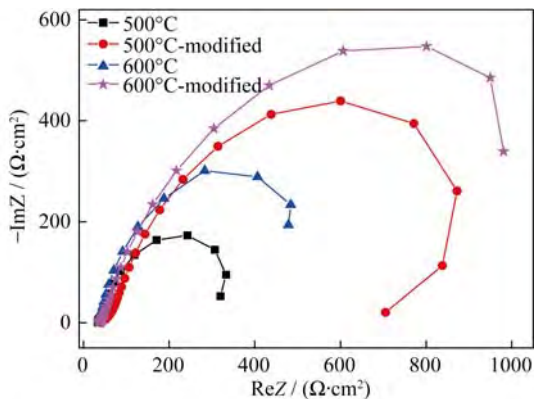


Fig. 5. Impedance spectra of the untreated and hydrophobic Fe–W deposition layer at different heat treatment temperatures.

4. Conclusions

Through a three-step coating process, we have developed hydrophobic films by incorporating micro-nano scale wire and protuberance structures on a Fe–W deposition layer. The 600°C annealed surface shows a higher contact degree ($(134 \pm 1)^\circ$). The average values of capacitance, roughness

factor, and impedance for the specific surface areas of the 600°C heat-treated sample are greater than those of the sample treated at 500°C. The hydrophobicity is strongly dependent on surface roughness and surface energy. Moreover, the hydrophobic samples have a better corrosion resistance than the untreated samples. These results are instrumental in extending the applications of amorphous electroplated depositions and shed light on further surface modifications.

Acknowledgements

This research was financially supported by the National Magnetic Confinement Fusion Science Program (No. 2010GB106003) and the National Natural Science Foundation of China (No. 91023037).

References

- [1] E. Richard, S.T. Aruna, and B.J. Basu, Superhydrophobic surfaces fabricated by surface modification of alumina particles, *Appl. Surf. Sci.*, 258(2012), No. 24, p. 10199.
- [2] C. Zhang, Y. Wu, and L. Liu, Robust hydrophobic Fe-based amorphous coating by thermal spraying, *Appl. Phys. Lett.*,

- 101(2012), No. 12, art. No. 121603.
- [3] L. Li, V. Breedveld, and D.W. Hess, Creation of superhydrophobic stainless steel surfaces by acid treatments and hydrophobic film deposition, *ACS Appl. Mater. Interfaces*, 4(2012), No. 9, p. 4549.
- [4] H.Z. Chen, X. Zhang, P.Y. Zhang, and Z.J. Zhang, Facile approach in fabricating superhydrophobic SiO₂/polymer nanocomposite coating, *Appl. Surf. Sci.*, 261(2012), p. 628.
- [5] A.C.C. de Leon, R.B. Pernites, and R.C. Advincula, Superhydrophobic colloidal textured polythiophene film as superior anticorrosion coating, *ACS Appl. Mater. Interfaces*, 4(2012), No. 6, p. 3169.
- [6] X.M. Zheng, Q.B. Zhang, and J. Wang, Fabrication of superhydrophobic magnetic Fe/SiO₂ surface with tunable adhesion inspired by lotus leaf, *Micro Nano Lett.*, 7(2012), No. 6, p. 561.
- [7] F. Song, H.L. Su, J. Han, D. Zhang, and Z.X. Chen, Fabrication and good ethanol sensing of biomorphic SnO₂ with architecture hierarchy of butterfly wings, *Nanotechnology*, 20(2009), No. 49, p. 495502.
- [8] E. Chibowski, L. Hołysz, K. Terpilowski, and M. Jurak, Investigation of superhydrophobic effect of PMMA layers with different fillers deposited on glass support, *Colloids Surf. A*, 291(2006), No. 1-3, p. 181.
- [9] T. Darmanin, E.T. de Givenchy, S. Amigoni, and F. Guittard, Superhydrophobic surfaces by electrochemical processes, *Adv. Mater.*, 25(2013), No. 10, p. 1378.
- [10] S.H. Wang, X.W. Guo, Y.J. Xie, L.H. Liu, H.Y. Yang, R.Y. Zhu, J. Gong, L.M. Peng, and W.J. Ding, Preparation of superhydrophobic silica film on Mg–Nd–Zn–Zr magnesium alloy with enhanced corrosion resistance by combining micro-arc oxidation and sol–gel method, *Surf. Coat. Technol.*, 213(2012), p. 192.
- [11] E.K. Kim, J.Y. Kim, and S.S. Kim, Significant change in water contact angle of electrospray-synthesized SiO₂ films depending on their surface morphology, *Surf. Interface Anal.*, 45(2013), No. 2, p. 656.
- [12] Y. Liu, X.M. Yin, J.J. Zhang, Y.M. Wang, Z.W. Han, and L.Q. Ren, Biomimetic hydrophobic surface fabricated by chemical etching method from hierarchically structured magnesium alloy substrate, *Appl. Surf. Sci.*, 280(2013), p. 845.
- [13] S. Wang, Y.H. Ling, P. Zhao, N.Z. Zang, J.J. Wang, S.B. Guo, J. Zhang, and G.Y. Xu, Bonding tungsten, W–Cu-alloy and copper with amorphous Fe–W alloy transition, *Fusion Eng. Des.*, 88(2013), No. 4, p. 248.
- [14] J. Jia, J.F. Fan, B.S. Xu, and H.B. Dong, Microstructure and properties of the superhydrophobic films fabricated on magnesium alloys, *J. Alloys Compd.*, 554(2013), p. 142.
- [15] Y.H. Ling, J.S. Liao, X.Y. Liu, X.M. Wu, and X.D. Bai, Enhanced hydrogen production on porous TiO₂ nanotube arrays, *J. Nanosci. Nanotechnol.*, 10(2010), No. 11, p. 7020.
- [16] S. Levine and A.L. Smith, Theory of the differential capacity of the oxide/aqueous electrolyte interface, *Discuss. Faraday Soc.*, 52(1971), p. 290.